NJC

Accepted Manuscript

This is an *Accepted Manuscript*, which has been through the Royal Society of Chemistry peer review process and has been accepted for publication.

Accepted Manuscripts are published online shortly after acceptance, before technical editing, formatting and proof reading. Using this free service, authors can make their results available to the community, in citable form, before we publish the edited article. We will replace this *Accepted Manuscript* with the edited and formatted *Advance Article* as soon as it is available.

You can find more information about *Accepted Manuscripts* in the Information for Authors.

Please note that technical editing may introduce minor changes to the text and/or graphics, which may alter content. The journal's standard Terms & Conditions and the Ethical guidelines still apply. In no event shall the Royal Society of Chemistry be held responsible for any errors or omissions in this *Accepted Manuscript* or any consequences arising from the use of any information it contains.

ROYAL SOCIETY OF CHEMISTRY

www.rsc.org/njc

Journal Name

ARTICLE

Influence of Terminal Donor on the Performance of 4, 8-Dialkoxybenzo [1,2-b:4,5']dithiophene based Small Molecules for Efficient Solution-processed Organic Solar Cells

Received 00th January 20xx,
Accepted 00th January 20xx

DOI: 10.1039/x0xx00000x

www.rsc.org/

Sushil S. Bagde,[a] Hanok Park[a], Song-Mi Lee[a] and Soo-Hyoung Lee [a,*]

Two π–conjugated small molecules, BDT(TTBT)$_2$ and BDT(PTBT)$_2$ based on benzodithiophene (BDT) and benzothiadiazole (BT) substituted with different terminal groups such as hexyl-bithiophene and hexylphenyl-thiophene are investigated for use in solution-processed organic solar cells (OSCs). Investigations into the molecules reveal that variation of the terminal groups not only influences the optical and electronic properties, but also affects the crystallization and morphology of the small molecules. The BDT(TTBT)$_2$ device showed a power conversion efficiency (PCE) of 1.73% as a consequence of deep HOMO (V_{oc} = 0.81V), improved charge delocalization, and stronger light absorption (J_{sc} = 4.75 mA/cm^{-2}) when mild annealing was used as a result of improved texturing structures in morphology, while the BDT(PTBT)$_2$ device rather showed moderate PCE of 1.22% with J_{sc} of 2.88 mA/cm^{-2}, V_{oc} of 0.81 V, and FF of 0.52.

Introduction

Since low-cost energy conversion devices are a prime requirement of today's globalized era, solution–processed organic solar cells (OSCs) are seeking more attention in the research community due to their potential as a green energy technology and features like low cost, light weight, and high mechanical flexibility.[1-4] With perpetual efforts over the years, significant improvement has been made in polymer-based solar cells (PSCs) with bulk heterojunction (BHJ) architecture due to improved device structure, novel light absorbing photoactive materials with phase separated morphology and fabricating techniques, power conversion efficiencies (PCE) have reached 10%.[5-7] On the other side, solution-processed small molecules organic solar cells (SMOSCs) have equally placed themselves by showing promising efficiencies with ~7-8 % for BHJ solar cells, which is surely narrowing the performance gap with PSCs.[8-11] In comparison to polymeric donors, small molecules have distinct advantages like well-defined structure, facile synthesis and easy purification, which ultimately results in consistency in batch to batch synthesis. Additionally high V_{oc} and hole mobility can be obtained due to energy level tuning via a molecular engineering and novel design implementation in the photoactive layer.[7-8, 12]

Although SMOSCs are behind polymeric counterparts in their overall PCE, various lessons learned from BHJ PSCs can be applied to SM BHJ devices to improve their performance.[13] Similar to PSCs, donor materials used in the photoactive layer is the key component for obtaining the higher PCE in SMOSCs. To address this issue, several small molecules with different central donor core (D) units, such as dithieno (3,2-b;2',3'd) silole (DTS)[14], dithieno[3,2b:2',3'd] pyrroles (DTP)[15], naphtha[1,2-b:5,6-b'] dithiophene (NDT)[16] and benzo[1,2-b:4,5-b] dithiophene (BDT)[11], are developed with π-electron acceptors to make the D-A backbone structure, since D-A structure gives strong absorptions at longer wavelengths owing to effective charge transfer characteristics.[10] Among the donor core units, many efforts were devoted for the development of dialkoxy- and dialkyl-BDT based small molecules, as BDT motifs have symmetrical and planar π-conjugated structure, which can promote ordered π-π stacking and high hole mobility. For instance, Chen *et al*. reported BDT based small molecules having 2-ethylhexoxy substituted BDT as a central core with octyl cyanoacetate and 3-ethylrhodanine as a terminal donor, in which PCE of 7.38 % was obtained for DR3TBDT.[10] Further a new BDT based small molecule donor (DR3TBDTT) was reported by introducing thiophene or bithiophene moiety at the 4- and 8-positions of the BDT unit to obtain greater

[a] School of Semiconductor and Chemical Engineering, Chonbuk National University, Duckjin-dong 664-14, Jeonju 561-756, Republic of Korea.
Electronic supplementary information (ESI) available: Including structural characterizations and Fig. S1-S4

conjugation length and high J_{sc}, which delivered the highest PCE of 8.12 % among BDT based small molecules.[11]

Though there are several studies reported on modulation of molecular properties and structure-property relationship for molecular photovoltaics' material, [17-19] the mystery of designing a compound that would achieve high performance is still unsolved. Most of the studies are confined to investigating of different donor groups, acceptor groups, or their combination, [20] which also includes side chain engineering.[21] Limited attention has been given to the variation of terminal group and their influence on the performance of molecular photovoltaics. We recently reported D-π-A conjugated small molecule donor $BDT(TBT)_2$, consisting of a dialkoxy BDT unit as central donor core with triphenylamine terminated benzothiazole(BT) as an acceptor.[22] To further study the effect of terminal donor group variation on photoactive material, we prepared D-π-A conjugated small molecules, namely $BDT(PTBT)_2$ and $BDT(TTBT)_2$ by replacing the propeller triphenyl-amine (TPA) terminal donor unit with a hexylphenyl-thiophene (PT) or hexyl-bithiophene (TT) group (Fig.1). Phenyl and thiophene were selected for their varying degrees of planarity and their quinoidal character, [23] which would affect their propensity of π-stacking with another molecular framework leading to enhanced charge transport between the adjacent molecules. In the present investigation, we focused on the effect of terminal donor group variations (PT and TT) on absorption, energy level, charge transport, morphology and photovoltaic properties of these small molecules. It was expected that the end-group and resultant planarity of molecules would influence the optical and morphological properties of the small molecules, hence the efficiency of the corresponding solar cells. SMOSCs' based on $BDT(TTBT)_2$ exhibited PCE of 1.73% with J_{sc} of 4.75 mA/cm^2, V_{oc} of 0.81V and FF of 0.45, whereas a relatively lower PCE of 1.22% was observed for $BDT(PTBT)_2$ with J_{sc} of 2.88 mA/cm^2, V_{oc} of 0.81V, and *FF* of 0.52.

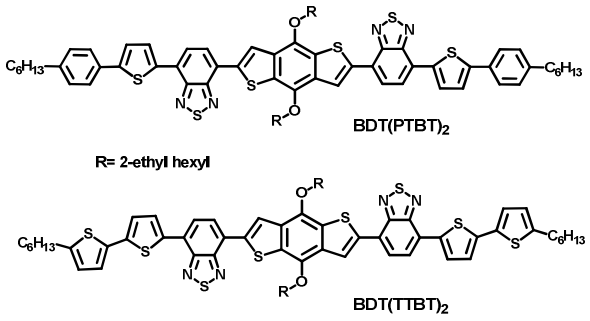

Fig. 1 Chemical structures of small molecules.

Experimental section

Materials

2-(4-Hexylphenyl)-thiophene(3): In a 50 mL flame-dried flask1-bromo-4-hexylbenzene (0.5 g, 2.07 mmol), tributyl(thiophen-2-yl)stannane (0.92 g, 2.48 mmol), and Pd $(PPh_3)_4$ (0.11 g, 0.10 mmol) were added and subjected to three vacuum/nitrogen (N_2) filled cycles. Subsequently, N_2- degassed toluene (10 mL) was added. The reaction mixture was heated to reflux for 24 h and monitored by thin-layer chromatography. After the completion, the reaction was quenched with water and the organic layer was extracted with dichloromethane. The solvent was removed under reduced pressure. The resulting crude was purified by column chromatography, eluting with hexane to obtain compound 3 (0.48 gm, 96%) a colorless liquid. ^{1}H NMR (400 MHz. $CDCl_3$, ppm) δ: 7.53-7.51 (d, 2H), 7.31-7.29 (m, 2H), 7.27-7.23 (d, 2H), 7.19-7.07 (m,1H) 2.6 (t, 2H), 1.6 (m, 2H), 1.36-1.31 (m, 6H), 0.9 (t, 3H). ^{13}C NMR ($CDCl_3$, 100 MHz, ppm) δ: 144.61, 142.42, 131.83, 128.88, 127.96, 127.88, 127.44, 125.95, 125.86, 124.77, 124.23, 123.05, 122.55, 35.63, 31.71, 31.35, 28.96, 22.59, 14.07.

5-(4-Hexylphenyl)thiophen-2-yl) trimethylstannane(4) : A stirred solution of 2-(4-hexylphenyl)thiophene (0.1 g, 0.409 mmol) in dry THF was cooled to – 78 ^{0}C under N_2, and n-BuLi (0.19 mL, 1.2 eq., 2.2 M in hexane) was added dropwise. The reaction mixture was stirred at –78 ^{0}C for another 1 hr, and subsequently Bu_3SnCl (0.49 mL, 1.2 eq) was added. The reaction mixture was allowed to warm to room temperature overnight with stirring. The reaction was then poured into H_2O (10 mL), and extracted with Et_2O. The organic layer was combined and dried over $MgSO_4$, and the solvent was removed under reduced pressure. The crude (0.13 g, 78%)was used for further reaction. ^{1}H NMR (400 MHz. $CDCl_3$, ppm) δ: 7.43-7.4 (m, 3H), 7.07-7.04 (m, 3H), 2.49 (t, 2H), 1.5 (m, 2H), 1.28-1.12 (m, 6H), 0.79 (t, 3H), 0.29 (s, 9H). ^{13}C NMR ($CDCl_3$, 100 MHz, ppm) δ: 144.59, 142.40, 136.08, 131.82, 128.87, 128.80, 127.96, 127.87, 125.93, 125.84, 124.22, 123.86, 122.53, 45.74, 35.61, 31.70, 31.35, 28.94, 22.59, 14.09, -8.2.

4-Bromo-7-(5'-hexyl-2,2'-bithiophen-5-yl)benzo[c][1,2,5] thiadiazole (6) : In a 50 mL flame-dried two-necked flask, 2-(5-(5-hexylthiophen-2-yl)thiophen-2-yl)-4,4,5,5-tetramethyl1,3, 2-dioxaborolane (0.2 g, 0.53 mmol), 4,7-dibromobenzo[c][1, 2, 5]thiadiazole (0.15 g, 0.53 mmol), and $Pd(PPh_3)_4$ (0.03 g, 0.02 mmol) were added and subjected to three vacuum/(N_2) filled cycles. N_2 degassed toluene (10 mL) and an aqueous 2M K_2CO_3 were added. The reaction was heated to reflux for 24 h and was monitored by thin-layer chromatography. Water was added to quench the reaction and organic layer was extracted with dichloromethane. Solvent was removed under reduced pressure. The resulting crude was purified using column chromatography, eluting with hexane/chloroform (4:6) to obtain compound 6 as a red coloured solid (0.11 g, 45%). ^{1}H NMR (400 MHz. $CDCl_3$, ppm) δ: 8.02 (d, 1H), 7.85 (d, 1H), 7.69 (d, 1H), 7.18 (d, 1H), 7.11 (d, 1H), 6.72 (d, 1H), 2.81 (t, 2H), 1.7 (m, 2H), 1.33-1.25 (m, 6H), 0.9 (t, 2H). ^{13}C NMR ($CDCl_3$, 100 MHz, ppm) δ: 153.77, 151.62, 146.28, 139.90, 136.90, 136.35, 134.31, 132.24, 128.86, 126.86, 125.02,

124.97, 123.94, 123.78, 111.90, 31.53, 31.52, 30.20, 29.67, 28.74, 22.54, 14.06.

4-Bromo-7-(5-(4-hexylphenyl)thiophen-2-yl)benzo[c][1,2,5] thiadiazole (7): In a 50 mL flame- dried flask, 4,7-dibromobenzo[c][1,2,5]thiadiazole (0.688 g, 2.34 mmol), (5-(4-hexylphenyl)thiophen-2-yl)trimethylstannane (1.33 g, 3.28 mmol), $Pd_2(dba)_3$ (18.69 mg, 3 mol %), and P(o-tolyl)$_3$ (20.7 mg, 10 mol %) were added and subjected to three vacuum/N_2 filled cycles. Subsequently N_2-degassed chlorobenzene (15 mL) was added, and the mixture was stirred for 15 min with flushing N_2. The reaction mixture was heated to reflux for 24 h, and was monitored by thin-layer chromatography. After completion of the reaction, chlorobenzene was removed under reduced pressure, and the residue was purified by column chromatography, eluting with hexane/chloroform (3:7) to obtain compound 7 (0.31 g, 29%) as a yellow solid. ^{1}H NMR (400 MHz. $CDCl_3$, ppm) δ: 8.05 (d, 2H), 7.81 (d, 1H), 7.73 (d, 1H), 7.59 (d, 1H), 7.33 (d, 1H), 7.22 (d, 2H), 2.6 (t, 2H), 1.67-1.57 (m, 2H), 1.37-1.25 (m, 6H), 0.89 (s, 3H). ^{13}C NMR ($CDCl_3$, 100 MHz, ppm) δ: 153.78, 151.67, 146.36, 143.12, 137.09, 132.25, 131.30, 129.18, 128.99, 127.07, 125.72, 125.67, 125.17, 123.61, 111.94, 35.68, 31.70, 31.32, 28.90, 22.59, 14.08.

BDT(TTBT)$_2$: In a 50 mL flame-dried flask, 2,6-bis(trimethyltin)-4,8-bis-(ethylhexyloxy) benzo[1,2-b:4,5-b] dithiophene **8** (0.1 g, 0.129 mmol), 4-bromo-7-(5'-hexyl-2,2'-bithiophen-5-yl)benzo[c][1, 2, 5] thiadiazole **6** (0.132 g, 0.284 mmol), $Pd_2(dba)_3$ (5.9 mg, 5 mol %) and P(o-tolyl)$_3$ (3.9 mg, 10 mol %) were added and subjected to three vacuum/ N_2 filled cycles. Subsequently N_2-degassed chlorobenzene (8 ~~ml~~ mL) was added, and the mixture was stirred for 15 min with flushing N_2. The reaction mixture was heated to reflux for 24 h, and was monitored by thin-layer chromatography. After completion of the reaction, chlorobenzene was removed under reduced pressure, and the residue was purified by column chromatography, eluting with hexane/chloroform (2:3) to obtain BDT(TTBT)$_2$ (0.11 g, 70%) as a violet solid. ^{1}H NMR (400 MHz. $CDCl_3$ ppm) δ: 8.57 (s, 2H), 7.9 (d, 2H), 7.6 (d, 4H), 6.9 (d, 4H), 6.7 (d, 2H), 4.21 (d, 4H), 2.22 (t, 4H), 1.9-1.34 (m, 6H), 1.25-1.14 (m, 28H), 1.04 (t, 6H), 0.9 (t,12H). ^{13}C NMR ($CDCl_3$, 100 MHz, ppm) δ: 152.49, 152.28, 145.9, 144.42, 139.45, 138.55, 137.15, 134.56, 133.19, 128.99, 128.27, 126.85, 126.04, 125.07, 124.78, 124.45, 123.55, 123.49, 121.95, 40.82, 31.61, 31.46, 30.71, 30.21, 29.72, 29.45, 28.87, 24.04, 23.36, 22.62, 14.41, 14.11, 11.64.

BDT(PTBT)$_2$: In a 50 mL flame-dried flask, 2,6-bis(trimethyltin)-4,8-bis-(ethylhexyloxy) benzo[1,2-b:4,5-b] dithiophene **8** (0.081 g, 0.104 mmol), 4-bromo-7-(5-(4-hexylphenyl)thiophen-2-yl)benzo[c][1,2,5] thiadiazole **7** (0.105 g, 0.230 mmol), $Pd_2(dba)_3$ (4.8 mg, 5 mol %), and P(o-tolyl)$_3$ (3.19 mg,10 mol %) were added and subjected to three vacuum/ N_2 filled cycles. Subsequently N_2-degassed chlorobenzene (8 mL) was added, and the mixture was stirred for 15 min with flushing N_2. The reaction mixture was heated to reflux for 24 h, and was monitored by thin-layer chromatography. After completion of the reaction, chlorobenzene was removed under reduced pressure, and the residue was purified by column chromatography, eluting with hexane/chloroform (2:3) to obtain BDT(PTBT)$_2$ (0.75g, 60%) as a purple solid. ^{1}H NMR (400 MHz. $CDCl_3$ ppm) δ: 8.54 (s, 2H), 7.89 (d, 2H), 7.63 (d, 4H), 7.45-7.43 (m, 4H), 7.14-7.08 (d, 6H), 4.2 (d, 4H), 2.55 (t, 4H), 1.87-1.30 (m, 6H), 1.25-1.14 (m, 28H), 1.05 (t, 6H), 0.89 (t, 12H). ^{13}C NMR ($CDCl_3$, 100 MHz, ppm) δ: 152.49, 152.33, 145.76, 144.40, 142.73, 138.74, 137.88, 133.17, 131.38, 128.95, 128.79, 128.60, 126.80, 126.21, 125.47, 125.16, 124.56, 123.28, 121.95, 40.85, 35.68, 31.76, 31.26, 30.74, 29.49, 29.07, 24.08, 23.38, 22.65, 14.52, 14.41, 14.11, 11.65.

General instrumentation

Chemical shifts were reported as δ values (ppm) relative to the internal standard tetramethylsilane (TMS). The UV-Vis absorption spectra films or solutions were obtained using a Shimadzu UV-2550 spectrophotometer. Photoluminescence (PL) spectra of films were obtained using an FP-6500 (JASCO). Thermogravimetric analysis (TGA) was carried out with a TA Instrument Q-50 at a scanning rate of 10 ^{O}C min^{-1} under N_2 atmosphere. Differential scanning calorimetry (DSC) experiments were performed on a TA Instrument (DSC 2910) at a heating rate of 100 ^{O}C min^{-1} under a N_2 atmosphere. Cyclic voltammetry (CV) measurements were taken by a VersaSTAT3 (METEK) Electrochemical Analyser under argon at a scan rate of 50 mV s^{-1} at room temperature, where a Pt wire and Ag/ AgCl were used as the counter- and reference electrodes, respectively. The reference electrode was calibrated with ferrocene/ ferrocenium (Fc/Fc+) redox couple (4.4 eV below the vacuum level) as an external standard. The samples were prepared in chloroform solution with 0.10M tetrabutylammonium hexafluorophosphate (n-Bu_4NPF_6) as the

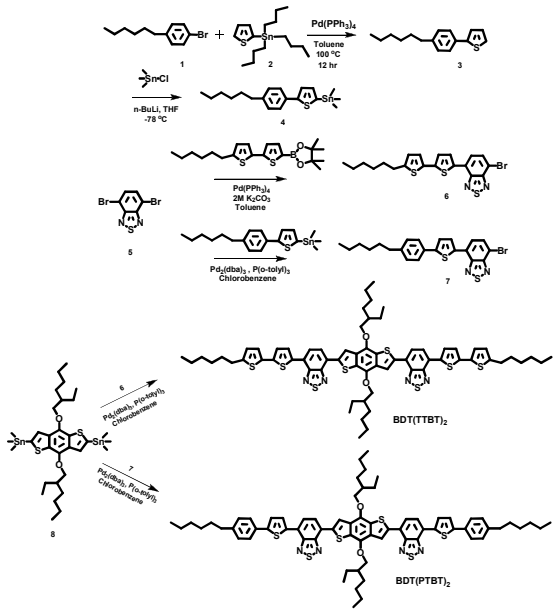

Scheme 1 Synthesis route of $BDT(TTBT)_2$ and $BDT(PTBT)_2$

electrolyte. The surface morphology was measured using a Digital Instruments Multimode atomic force microscope (AFM) controlled by a Nanoscope IIIa scanning probe microscope 20 controller.

Photovoltaic device fabrication and characterization

OSCs comprising a BHJ photoactive layer of small molecules: 6, 6- phenyl-C_{71}–butyric acid methyl ester ($PC_{71}BM$) were prepared on a commercial indium-doped tin oxide (ITO)-coated glass substrate with a sandwiched structure of glass/ ITO/PEDOT: PSS/ $BDT(PTBT)_2$ or $BDT(TTBT)_2$:$PC_{71}BM$/ LiF/Al. Prior to use, the patterned ITO-coated glass substrates were cleaned with deionized water, acetone, and isopropyl alcohol using ultrasonication, followed by treatment with UV ozone. Poly(3,4-ethylenedioxythiophene): poly(styrene sulfonate) (PEDOT:PSS) (AI 4083, H. C. Starck) was spin-coated (2600 rpm, 40 s) onto the cleaned ITO-glass at a thickness of 40 nm and dried at 140 ^{O}C for 20 min in atmosphere and then transferred into a glove box filled with N_2. Blends of $BDT(PTBT)_2$ or $BDT(TTBT)_2$ and $PC_{71}BM$ (Nano-C, USA) with different weight ratios (from 1:1 to 1:4 w/w) were solubilized overnight in chlorobenzene (20 mg mL^{-1}) filtered through a 0.45 mm poly(tetrafluoroethylene) (PTFE) filter and subsequently spin-coated (thickness, 60–70 nm) onto the PEDOT:PSS layer of the ITO. The resulting films were dried at room temperature for 20 min under N_2 and then under vacuum for 12 h. The devices were completed by deposition of a 0.5 nm layer of LiF and a 120 nm Al layer. These layers were thermally evaporated at room temperature under high vacuum at 1×10^{-6} Torr. The active area of every device was 9 mm^2. The current density–voltage (*J–V*) characteristics of the photovoltaic devices were measured in the dark and under 1 sun illumination at AM 1.5G using a solar simulator (Newport) at 100 mW cm^{-2} adjusted with a standard PV reference (2×2 cm^2), a mono-crystalline silicon solar cell (calibrated at NREL, Colorado, USA) with a Keithley 2400 source-measure unit. The external quantum efficiency (EQE) was determined using a Polaronix K3100 spectrometer.

Results and discussion

Synthesis and structural characterization

The synthetic route of small molecules, $BDT(PTBT)_2$ and $BDT(TTBT)_2$ is depicted in Scheme 1. 2-(4-hexylphenyl)thiophene (3) was prepared via Pd-catalyzed stille coupling of 1-bromo-4-hexylbenzene (1) and tributyl(thiophen-

Table 1 The optical, electrochemical characteristics and hole/electron mobilities of small molecules.

Journal Name

ARTICLE

Molecule	λ_{max} [a] (nm)	λ_{max} [b] (nm)	E_g [c] (eV)	E^{ox}_{onset} [d] / HOMO (eV)	LUMO [e] (eV)	μ_h [f] ($cm^2 V^{-1} s^{-1}$)	μ_e [f] ($cm^2 V^{-1} s^{-1}$)
$BDT(TTBT)_2$	555	586,622	1.75	1.18/-5.58	-3.83	1.77×10^{-5}	1.08×10^{-4}
$BDT(PTTB)_2$	540	560,600	1.83	0.93/-5.33	-3.50	1.32×10^{-7}	8.71×10^{-5}

[a] Measured in chloroform solution. [b] Spin-coated film from chloroform solution. [c] Optical band gap, $E_g^{opt} = 1240/(\lambda_{onset})$film. [d] Potential determined by cyclic voltammetry in 0.10 M Bu_4NPF_6-CH_3CN. HOMO =-e(E^{ox}_{onset}+4.4). [e] LUMO = E_g + HOMO. [f] hole mobilities (μ_h) and electron mobility (μ_e) measured by SCLC technique.

2-yl)stannane (2). Lithiation of compound (3) with n-BuLi followed by quenching with trimethyltin chloride afforded (5-(4-hexylphenyl)thiophen-2-yl) trimethylstannane (4) in 78% yield. 4-bromo-7-(5-(4-hexylphenyl)thiophen-2-yl) benzo[c][1,2,5] thiadiazole (7) was obtained by selective Pd-catalyzed stille coupling between compound (4) and benzothiadiazole (5) in 29% yield. Similarly intermediate 4-bromo-7-(5'-hexyl-2,2'-bithiophen-5-yl) benzo [c] [1,2,5]thiadiazole (6) was obtained by Pd-catalysed Suzuki coupling between 2-(5'-hexyl-2,2'-bithiophen-5-yl)-4,4,5,5-tetramethyl-1,3,2-dioxaborolane and benzothiadiazole in 45% yield. 2,6-Bis(trimethyltin)-4,8-bis-(ethylhexyloxy) benzo[1,2-b:4,5-b] dithiophene (8) was prepared by following described procedure in the literature.[24] Desired final molecules were obtained by $Pd_2(dba)_3$/P(o-tolyl)$_3$ catalysed stille cross coupling of 8 and 6, $BDT(TTBT)_2$ was obtained as a violet solid in 70% yield, under the identical conditions by reacting 8 and 7 afforded $BDT(PTBT)_2$ as purple solid, in 60% yield. Structural characterizations are described in the experimental section of supporting information (SI). Differential scanning calorimetry (DSC) and thermal gravimetric analysis (TGA) were used to prove the properties and stabilities, respectively. TGA showed 5% weight loss up to 291°C and 320°C for $BDT(TTBT)_2$ and $BDT(PTBT)_2$ respectively indicating excellent thermal stability and long term utility. DSC was performed at a heating (cooling) scan rate of 10°C min^{-1} under N_2. DSC traces of $BDT(TTBT)_2$ and $BDT(PTBT)_2$ are shown in Fig.S1 and S2 (SI). Melting transitions were observed at 207°C and 275°C for $BDT(TTBT)_2$ and $BDT(PTBT)_2$ respectively. $BDT(TTBT)_2$ and $BDT(PTBT)_2$ showed crystallization temperatures at 188°C and 250°C, respectively. The higher melting point and crystallization temperature of $BDT(PTBT)_2$ may be attributed to tightly packed domains of the molecule, which likely favours compact intermolecular π-π conjugated structure. Hence, these results indicate that the subtle change in the end-groups of $BDT(TTBT)_2$ and $BDT(PTBT)_2$ significantly influence the molecular packing and crystalline behaviour.

Photophysical properties

The UV-visible optical absorption spectra of $BDT(TTBT)_2$ and $BDT(PTBT)_2$ in chloroform (10^{-5}M) and solid films spin-coated on a quartz substrate at room temperature are shown in Fig. 2, and corresponding data are summarized in Table 1. Both molecules display π-π* transitions at shorter wavelengths and intramolecular charge transfers (ICT) at the higher wavelengths. In solution, $BDT(TTBT)_2$ and $BDT(PTBT)_2$

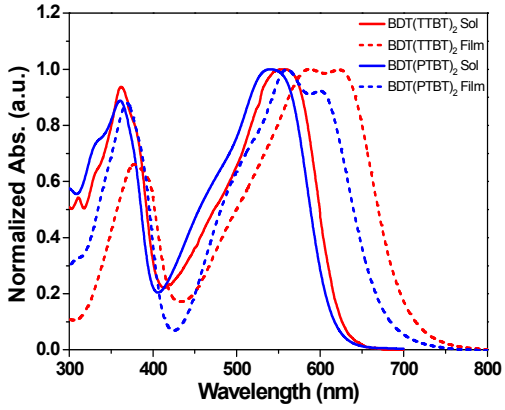

Fig. 2 Normalized UV-visible absorption spectra of $BDT(TTBT)_2$ and $BDT(PTBT)_2$ in chloroform solution and thin film at room temperature.

exhibited absorption maxima at 555 nm and 540 nm respectively, which were red shifted in thin films to 586 nm and 560 nm respectively. In a thin film absorption spectra, $BDT(TTBT)_2$ affords higher red shift of 31 nm along with the emergence of a well-defined vibronic splitting peak at 622 nm. Such features are attributed to a more rigid and ordered structure in the solid, which also lead to enhanced π-electron delocalization across the molecular backbone.[11] Whereas for $BDT(PTBT)_2$, relatively lower shift of 20nm with pronounced vibronic splitting with intense shoulder peak was observed. The difference in absorption shifts from solutions to films indicate that $BDT(TTBT)_2$ exhibits better molecular stacking than $BDT(PTBT)_2$. Improved vibronic resolution of the absorption of $BDT(TTBT)_2$ arise from a better molecular ordering and packing (more π-π stacking) in the thin film. Optical band gap (E_g^{opt}) of $BDT(TTBT)_2$ and $BDT(PTBT)_2$ in the thin films were calculated as 1.75eV and 1.83eV, respectively.

Electrochemical properties

Cyclic voltammetry (CV) measurements of both small molecules were carried out in 0.1M solutions of Bu_4NPF_6 in acetonitrile at room temperature under argon with scan rate of 50 mVs^{-1} to evaluate the electrochemical characteristics, and their highest occupied molecular orbital (HOMO) energy levels. As shown in Fig. 3a, the onset potential for the oxidation of $BDT(PTBT)_2$ and $BDT(TTBT)_2$ were located around 0.93V and 1.18V versus the Ag/AgCl reference electrode, hence the respective HOMO energy levels are -5.33 and -5.58 eV. These values were determined from corresponding E_{ox} onset according to the equation E_{HOMO}= -e (E^{ox}_{onset} + 4.4). $BDT(PTBT)_2$ showed a higher HOMO level, which could be the result of increased donor strength across the molecular backbone, afforded by the higher aromatic character of the terminal moiety.[24] The HOMO level of $BDT(TTBT)_2$ was about (0.25eV) lower than that of $BDT(PTBT)_2$, indicating that $BDT(TTBT)_2$ has more oxidation stability. Switching from phenyl-thiophene to bi-thiophene in $BDT(TTBT)_2$, lowered the HOMO energy level, and ensured the higher V_{oc} in the device, as it is linearly correlated with the difference between the HOMO of the donor and the lowest occupied molecular orbital (LUMO) of the acceptor.[25] The LUMO energy levels of the both small molecules were calculated based on the correlation between the optical band gap (E_g) and the HOMO energy level ($E_{LUMO} = E_g + E_{HOMO}$). Table 1 summarizes the corresponding electrochemical characteristics, including onset oxidation (E^{ox}_{onset}) and the estimated energy levels (both HOMO and LUMO) for the small molecules. The energy levels of $BDT(TTBT)_2$ and $BDT(PTBT)_2$ were further compared with that of $PC_{71}BM$ using the energy level diagram (Fig. 3b). The LUMO levels of $BDT(TTBT)_2$ and $BDT(PTBT)_2$ are sufficiently higher enough than the LUMO level of $PC_{71}BM$ to overcome the exciton binding energy and thus ensure an efficient exciton splitting and charge transfer.[26]

Photovoltaic properties

The photoactive layers (small molecule : $PC_{71}BM$) were

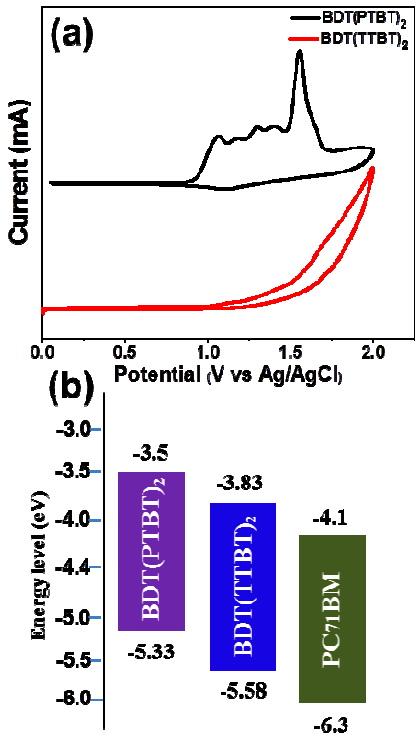

Fig. 3 a) Cyclic Voltammogram of small molecules. b) Energy level diagram showing the HOMO and LUMO energy level of small molecules with $PC_{71}BM$.

prepared in solutions of chlorobenzene (20mg/~~ml~~ mL). OSCs with active area of 9 mm^2 were tested in dark and under AM 1.5G (100$mWcm^{-2}$) illumination. A series of small molecules: $PC_{71}BM$ blend ratios were tested from 1:1 to 1:4 to get the optimal blend ratio for each small molecule, followed by thermal annealing in order to evaluate the device performance. The detailed device performance data is presented in Table 2. The current density-voltage (*J-V*) curve is provided in Figure 4a. The optimal blend ratios for $BDT(TTBT)_2$ and $BDT(PTBT)_2$ were found to be (1:2) and (1:4) respectively, to afford maximum PCEs. From the device based on $BDT(TTBT)_2$: $PC_{71}BM$ (1:2), a PCE of 1.67% with V_{oc} of 0.81V, J_{sc} of 4.25 mA/cm^2 and FF of 0.49 were found. Conversely, for $BDT(PTBT)_2$: $PC_{71}BM$ (1:4), relatively lower PCE of 1.14% with V_{oc} of 0.78V, J_{sc} of 2.85 mA/cm^2 and FF of 0.51 was recorded. The optimization of the solar cells was further carried out by applying thermal annealing conditions (90, 120, and 150°C) to the solar cell devices of $BDT(TTBT)_2$ and $BDT(PTBT)_2$, since thermal annealing can significantly influence the morphology of the active layers and consequently improve the performances of the photovoltaic devices.[27] Proceeding with thermal annealing, when the $BDT(TTBT)_2$: $PC_{71}BM$ (1:2) device was annealed at 90°C, an enhanced PCE of 1.73% with similar V_{oc} of 0.81V, improved J_{sc} of 4.75 mA/cm^2, and FF of 0.45 was obtained. This enhancement in PCE could be attributed to increased J_{sc} of the resultant device. When a similar strategy of thermal annealing at 90°C was

Journal Name

ARTICLE

Table 2 Summary of the photovoltaic characteristics of OSCs based on **BDT(TTBT)$_2$: PC$_{71}$BM** and **BDT(PTBT)$_2$: PC$_{71}$BM** devices

Molecule	ratio	TA	*Jsc* (mA/cm^2)	*Voc* (V)	FF	η (%)	Thickness(nm)
BDT(TTBT)$_2$:PC$_{71}$BM	1:1	-	3.81	0.81	0.46	1.40	60~65
	1:2		4.25	0.81	0.49	1.67	
	1:3		2.82	0.77	0.49	1.07	
	1:4		1.97	0.77	0.32	0.50	
	1:2	90℃ / 10m	4.75	0.81	0.45	1.73	
		120℃ / 10m	4.83	0.80	0.39	1.49	
		150℃ / 10m	4.36	0.74	0.32	1.04	
BDT(PTBT)$_2$:PC$_{71}$BM	1:1	-	2.02	0.83	0.39	0.65	
	1:2		2.32	0.81	0.33	0.62	
	1:3		2.71	0.80	0.49	1.07	
	1:4		2.85	0.78	0.51	1.14	
	1:4	90℃ / 10m	2.88	0.81	0.52	1.22	
		120℃ / 10m	2.61	0.78	0.40	0.82	
		150℃ / 10m	1.90	0.59	0.27	0.31	

applied for the BDT(PTBT)$_2$: PC$_{71}$BM (1:4) device, all the device parameters were elevated and PCE reached its peak value of 1.22% with improved J_{sc} of 2.88 mA/cm^2, V_{oc} of 0.81V, and FF of 0.52. The further increment in annealing temperature was found to be ineffective, as PCEs drastically dropped in both small molecules. For BDT(TTBT)$_2$: PC$_{71}$BM (1:2), annealing at 120^{o}C and 150^{o}C showed PCEs of 1.49% and 1.04% respectively, with concomitant decrease in V_{oc}, J_{sc} and FF, whereas steep decrease in PCE was observed for BDT(PTBT)$_2$: PC$_{71}$BM (1:4) with an incresae in annealing temperature from 120^{o}C to 150^{o}C; PCE dropped from 0.82% to 0.32% respectively, with all device parameters decreased.

To investigate the devices' photoresponses, external quantum efficiency (EQE) spectra of the devices based on BDT(TTBT)$_2$: PC$_{71}$BM (1:2) and BDT(PTBT)$_2$: PC$_{71}$BM (1:4) were collected under monochromatic light (Fig. 4b). The EQE curve showed spectral coverage in the region 350-650nm for both the molecules. BDT(TTBT)$_2$ devices exhibited broader coverage with a maximum of ~ 34% at ~380 nm, leading to a considerable increase in J_{sc}, Whereas, BDT(PTBT)$_2$ shows maxima of ~25% at ~360 nm. Reduced spectral coverage around 450-650 nm causes lower J_{sc} in BDT(PTBT)$_2$ devices.

Charge carrier mobility

The hole and electron mobilities of the small molecules were investigated by space-charge limited current (SCLC) method. Table 1 summarizes the resulting mobilities from measurements of the corresponding devices. The *J-V* characteristics of the hole only devices of small molecules, using device structure of ITO / PEDOT:PSS / small molecule:PC$_{71}$BM / MoO_3 / Ag, are shown in Fig. 5a. The hole mobility of the BDT(TTBT)$_2$: PC$_{71}$BM (1:2) film was calculated to be 1.77×10^{-5} cm^2 V^{-1} s^{-1}, which is 10^2 times higher than that of the BDT(PTBT)$_2$: PC$_{71}$BM (1:4) film (1.32×10^{-7} cm^2 V^{-1} s^{-1}). Furthermore, from the electron-only device with structure of ITO / ZnO / small molecule: PC$_{71}$BM / LiF / Al, the electron mobility of BDT(TTBT)$_2$: PC$_{71}$BM (1:2) was found to be 1.08×10^{-4} cm^2 V^{-1} s^{-1}, which is one order of magnitude higher than that of BDT(PTBT)$_2$: PC$_{71}$BM (1:4)

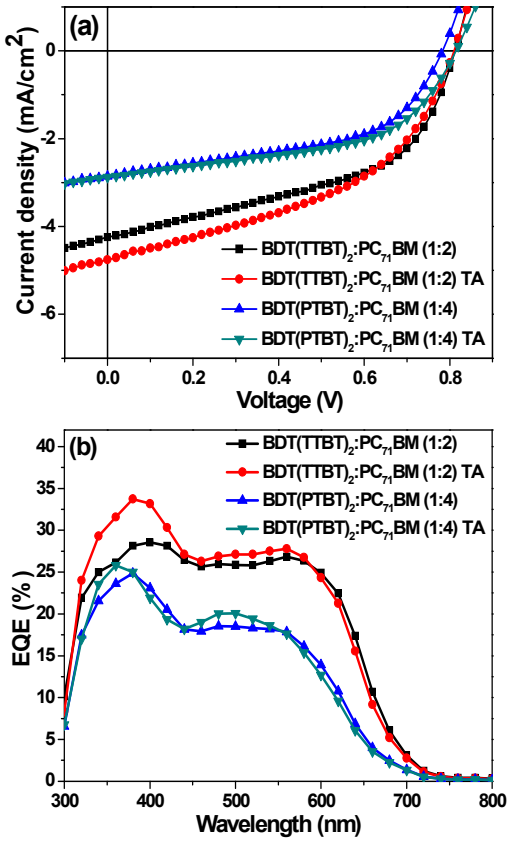

Fig. 4 a) J-V curves for solar cell devices based on small molecules: $PC_{71}BM$ blends. b) EQE spectra of solar cell devices based on small molecule: $PC_{71}BM$ blends.

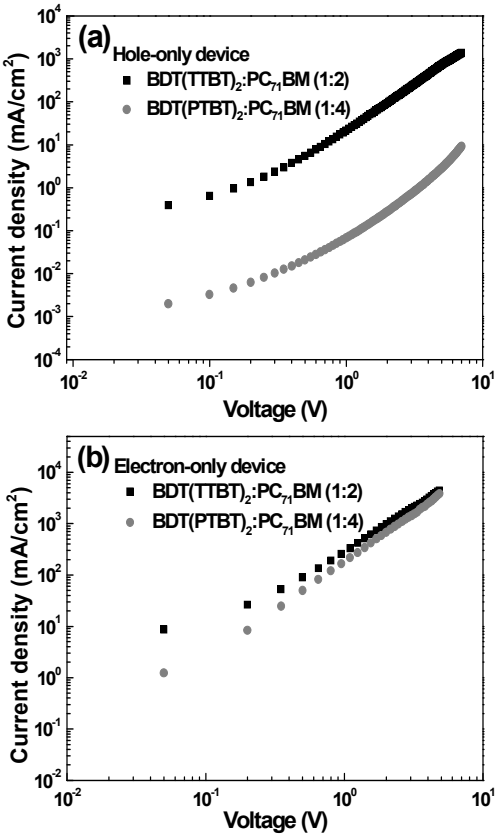

Fig. 5 Current density(*J*)-Voltage(*V*) characteristics of (a) hole- and (b) electron-only devices for BDT(TTBT)$_2$:PC$_{71}$BM(1:2) and BDT(PTBT)$_2$:PC$_{71}$BM(1:4).

(8.71×10^{-5} cm^2 V^{-1} s^{-1}) (Fig. 5b). The fact that the hole and electron mobility of BDT(TTBT)$_2$ is higher than that of the BDT(PTBT)$_2$ is obviously due to more chain-planarization and better molecular packing of BDT(TTBT)$_2$ molecule, which is also related with relatively higher PCE and J_{sc} values of BDT(TTBT)$_2$ based devices.

Thin –film morphology

The end-groups of BDT(TTBT)$_2$ and BDT(PTBT)$_2$ are expected to alter their miscibility with $PC_{71}BM$, which may influence the nano-scale morphology of the small molecule: $PC_{71}BM$ blend films. The active layer morphology of small molecules: $PC_{71}BM$ blends films were examined by an atomic force morphology (AFM) technique (Fig.S5 in SI). In BDT(TTBT)$_2$, an optimal photoactive blend ratio of 1:2 is required to obtain good compatibility of donor and acceptor phase. Whereas, in BDT(PTBT)$_2$, when excess $PC_{71}BM$ was used (1:4 ratio), it led to formation of desired interpenetrating network (IPN) that is sufficient for effective charge separation and carrier charge transport. Thus, for donors BDT(TTBT)$_2$ and BDT(PTBT)$_2$, higher photovoltaic performance was obtained for optimized photoactive blend ratios of 1:2 and 1:4 respectively. Further we characterized the BDT(TTBT)$_2$: $PC_{71}BM$ (1:2) and BDT(PTBT)$_2$: $PC_{71}BM$ (1:4) blended films with and without thermal annealing at 90^{o}C to investigate the relationship between the morphology and the device processing conditions of the optimized devices (Fig. 6). The AFM image of BDT(TTBT)$_2$: $PC_{71}BM$ (1:2) without thermal annealing shows distinct morphologies, which shows large interconnected domains with root mean square (RMS) roughness of 1.57nm (Fig. 6a). Whereas the BDT(PTBT)$_2$: $PC_{71}BM$ (1:4) blend film shows less phase separation morphology (Fig. 6c) with a similar RMS roughness value of 1.57 nm comparing with BDT(TTBT)$_2$: $PC_{71}BM$ film. In annealed film of BDT(TTBT)$_2$: $PC_{71}BM$ (1:2), texturing structure in morphology was observed with reduced RMS roughness of 1.03 nm, and gradual increase of fibrillary structure became more apparent (Fig. 6b). An optimized donor/acceptor (D/A) IPN may have been formed in the annealed film of BDT(TTBT)$_2$: $PC_{71}BM$ (1:2). This led to well
defined IPN structure, which ensured large D/A interface and efficient percolation channels for charge transport, thus improving the exciton separation and charge collection efficiency and leading to high J_{sc}. This also explain the high

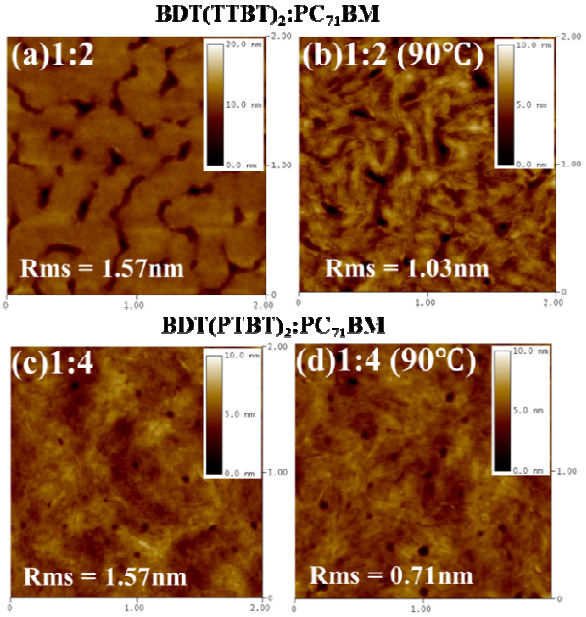

Fig. 6 AFM images of blend film spin-cast from a chlorobenzene solutions.

hole and electron mobility for this device.[28] On annealing, BDT(PTBT)$_2$: $PC_{71}BM$ (1:4) film showed much lower RMS roughness of 0.71nm (Fig. 6d). This could be because of high miscibility with $PC_{71}BM$, partly due to the improper orientation of molecular stacking in thin film. BDT(PTBT)$_2$: $PC_{71}BM$ (1:4) blend films shows homogeneous morphology without any distinct D/A interface, which could explain the reduced J_{sc} and charge mobility in the BDT(PTBT)$_2$ based device. Furthermore, from SCLC results, BDT(TTBT)$_2$: $PC_{71}BM$ (1:2) film exhibited more balanced hole and electron mobilities (μ_e/μ_h = 6.1) than that of BDT(PTBT)$_2$: $PC_{71}BM$ (1:4) (μ_e/μ_h = 660). This means that BDT(TTBT)$_2$: $PC_{71}BM$ (1:2) film has a better charge transporting ability towards the respective electrode. Consequently, this characteristic led to increased J_{sc} and thereby delivered a higher PCE for the BDT(TTBT)$_2$: $PC_{71}BM$ (1:2) device.

Conclusions

We developed two moderate bandgap small molecules, BDT(TTBT)$_2$ and BDT(PTBT)$_2$ with varied endgroups of hexyl-bithiophene or hexylphenyl-thiophene. Our study revealed that a small change of the terminal group in the small molecular donor materials impacts their optical, electrochemical, and morphological properties as well as the final photovoltaic performance of the solar cells. More ordered interchain molecular π- π stacking, broader spectral coverage from 350-700 nm were observed for BDT(TTBT)$_2$ due to its planar and enhanced conjugated system. As a consequence of high charge mobility ($\mu_h = 1.77\times10^{-5}$ cm^2 V^{-1} s^{-1}; $\mu_e = 1.08\times10^{-4}$ cm^2 V^{-1} s^{-1}), ordered crystalline morphology after blending with $PC_{71}BM$ and improved J_{sc} of 4.75 mA/cm^2, higher PCE of 1.73% was obtain for BDT(TTBT)$_2$. This enhancement increased PCE 1.4 times and J_{sc} 1.6 times compared to BDT(PTBT)$_2$ based devices (PCE= 1.22%, and J_{sc} of 2.88 mA/cm^2) respectively. Difference in the performance of photovoltaic performance of the molecules BDT(TTBT)$_2$ and BDT(PTBT)$_2$ demonstrates a rational design strategy for obtaining high performance photovoltaic materials via modification of terminal donor group.

Acknowledgements

This research was supported by Basic Science Research Program through the National Research Foundation of Korea (NRF) funded by the Ministry of Science, ICT and future planning (2015R1A2A2A01004404)

References

1) G. Li, V. Shrotriya, Y. Yao, J. Huang and Y. Yang, *J. Mater. Chem*, 2007, **17**, 3126
2) M. C. Scharber, D. Wuhlbacher, M. Koppe, P. Denk, C. Waldauf, A. J.Heeger, C. L. Brabec, *Adv. Mater*, 2006, **18**, 789.
3) Mishra, A.; Bauerle, P.¨ *Angew. Chem., Int. Ed*, 2011, **51**, 2020.
4) H. X. Zhou, L. Q. Yang, W. You, *Macromolecules* 2012, **45**, 607.
5) Y. Sun, G. C. Welch, W. L. Leong, C. J. Takacs, G. C. Bazan, A. J. Heeger, *Nat. Mater,* 2012, **11**, 44.
6) G. C. Welch, L. A. Perez, C. V. Hoven, Y. Zhang, X.D. Dang, A. Sharenko, M. F. Toney, E. J. Kramer, N. Thuc-Quyen, G. C. Bazan, *J. Mater. Chem*, 2011, **21**, 12700.
7) B. Walker, C. Kim, T. Q. Nguyen, *Chem. Mater*, 2011**, 23**, 470.
8) Y. M. Sun, G. C. Welch, W. L. Leong, C. J. Takacs, G.C. Bazan, A. J. Heeger, *Nat. Mater*, 2012, **11**, 44.
9) R. Fitzner, , E. Mena-Osteritz, A. Mishra, G. Schulz, E. Reinold, M. Weil, C. Körner, H. Ziehlke, C. Elschner, K. Leo, M. Riede, M. Pfeiffer, C. Uhrich, P. Bäuerle, *J. Am. Chem. Soc*, 2012, **134**, 11064.
10) J. Zhou, X. Wan, Y. Liu, Y. Zuo, Z. Li, G. He, G. Long, W. Ni, C. Li, X. Su, Y. Chen. *J. Am. Chem. Soc,* 2012, **134**, 16345.
11) J. Zhou, Y. Zuo, X.Wan, G. Long, Q.Zhang, W. Ni, Y. Liu, Z. Li, G. He, C. Li, B. Kan, M. Li, Y. Chen *J. Am. Chem. Soc,* 2013, **135**, 8484.
12) B. Walker, J. Liu, C. Kim, G.C. Welch, J. K. Park, J. Lin, P. Zalar, C. M. Proctor, J. H. Seo, G.C. Bazana, T.-Q. Nguyen, *Energy Environ. Sci,* 2013, **6**, 952.Y. Z. Lin, Y. F. Li, X. W. Zhan, *Chem. Soc. Rev,* 2012, **41**, 4245.
13) Y. Sun, G. C. Welch, W. L. Leong, C. J. Takacs, G. C. Bazan , A. J. Heeger, *Nat. Mater,* 2011, **11**, 44.

14) S. C. Rasmussen, S. J. Evenson, *Prog. Polym. Sci*, 2013, **38**, 1773.
15) S. Loser, H. Miyauchi, J. W. Hennek, J. Smith, C. Huang, A. Facchetti, T. J. Marks, *Chem. Commun,* 2012, **48**, 8511.
16) L. Huo,J , Hou, H.-Y. Chen, S. Zhang, Y. Jiang, T. L. Chen, Y. Yang, *Macromolecule,* 2009, **42**, 6564.
17) W. Li, W. S. C. Roelofs, M. M. Wienk, R. A. J. Janssen, *J. Am .Chem. Soc,* 2012, **134**, 13787.
18) P. Dutta, H. Park, M. Oh, S. Bagde, I. N. Kang, S.H. Lee, *J. Polym. Sci, Part A: Polym. Chem,* 2013, **51**, 2948.
19) L. Ye, S. Zhang, L. Huo, M. Zhang, J. Hou, *Acc. Chem. Res,* 2014, **47**, 1595.
20) Z.G. Zhang, S. Zhang, J. Min, C. Chui, J. Zhang, M. Zhang, Y. Li, *Macromolecules,* 2012, **45**, 113.
21) P. Dutta, J. Kim, S. H. Eom, W.H. Lee, I. N. Kang, S.H. Lee, *ACS Appl. Mater. Interfaces*, 2012, **4**, 6669.
22) H. J. Son, F. He, B. Carsten, L. Yu, *J. Mater. Chem*, 2011, **21**, 18934.
23) Y. Liang, D. Feng, Y. Wu, S. T. Tsai, G. Li, C. Ray, L. Yu, *J. Am. Chem. Soc*, 2009, **131**, 7792.
24) M. C. Scharber, D. Mühlbacher, M. Koppe, P. Denk, C. Waldauf, A. J. Heeger, C. J. Brabec, *Adv. Mater*, 2006, **18**, 789.
25) Y. He, H.Y. Chen, J. Hou, Y. Li, *J. Am. Chem. Soc,* 2010, **132**, 1377.
26) Y.J. Kim, M.J. Kim, T. K. An, Y.H. Kim, C. E. Park, *Chem.Commun.,* 2015, **51**, 11572.
27) J. Liu, B. Walker, A. Tamayo, Y. Zhang, T.-Q. Nguyen, *Adv. Funct. Mater,* 2013, **23**, 47.
28) Q. Zhang, B. Kan, F. Liu, G. Long, X. Wan, X. Chen, Y. Zuo, W. Ni, H. Zhang, M. Li, Z. Hu, F. Huang, Y. Cao, Z. Liang, M. Zhang, T. P. Russell, Y. Chen, *Nature Photons*, 2015, **9**, 35.

Graphical Abstract

Influence of Terminal Donor on the Performance of 4, 8-Dialkoxybenzo [1,2-b:4,5']dithiophene based Small Molecules for Efficient Solution-processed Organic Solar Cells

Sushil.S. Bagde,[a] Hanok Park[a], Song-Mi Lee[a] and Soo-Hyoung Lee[a,] *

[a]School of Semiconductor and Chemical Engineering, Chonbuk National University, Duckjin-dong 664-14, Jeonju 561- 756, Republic of Korea

*Corresponding author; Telephone: +063-270-2435, Fax: +063-270-2306,
E-mail: shlee66@jbnu.ac.kr

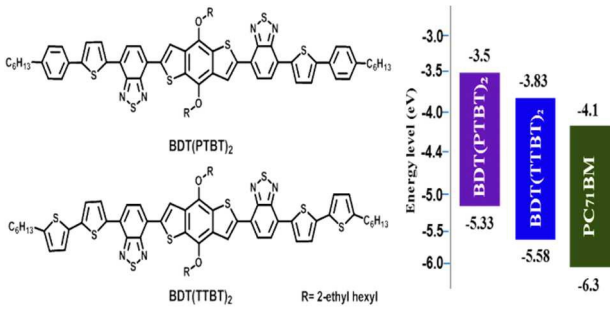

New dialkoxybenzo [1,2-b:4,5']dithiophene based small molecues, $BDT(PTBT)_2$ and $BDT(TTBT)_2$ are design and synthesized. $BDT(TTBT)_2$ shows higher PCE than $BDT(PTBT)_2$.